



The earliest beetle †*Coleopsis archaica* (Insecta: Coleoptera) – morphological re-evaluation using Reflectance Transformation Imaging (RTI) and phylogenetic assessment

Mario Schädel¹, Margarita I. Yavorskaya¹, Rolf Georg Beutel²

¹ Institut für Evolution und Ökologie, University of Tübingen, Auf der Morgenstelle 28, 72076 Tübingen, Germany

² Institut für Zoologie und Evolutionsforschung, Entomology Group, Friedrich Schiller University, Vor dem Neutor 1, 07743 Jena, Germany

<http://zoobank.org/6D2B8B22-07F7-4E61-8A21-E40FEC328BEA>

Corresponding author: Mario Schädel (mario.schaedel@gmail.com)

Received 15 May 2022

Accepted 3 July 2022

Published 14 September 2022

Academic Editor Martin Fikáček

Citation: Schädel M, Yavorskaya MI, Beutel RG (2022) The earliest beetle †*Coleopsis archaica* (Insecta: Coleoptera) – morphological re-evaluation using Reflectance Transformation Imaging (RTI) and phylogenetic assessment. *Arthropod Systematics & Phylogeny* 80: 495–510. <https://doi.org/10.3897/asp.80.e86582>

Abstract

The earliest known fossil beetle †*Coleopsis archaica* is re-examined using Reflectance Transformation Imaging (RTI). The morphological observations are evaluated with respect to phylogenetic implications and the early evolution of Coleoptera. †*Coleopsis archaica* belongs to an early Permian branch of beetles, outside a monophyletic unit comprising Coleoptera (in the widest sense) excluding †Tshekardocoleidae. This clade is mainly characterized by a complex of apomorphic features: elytra with epipleura and with a close fit with the posterior body, thus forming a tightly sealed subelytral space. In contrast to this, the elytra of †*C. archaica* and †Tshekardocoleidae cover the metathorax and abdomen in a loose tent-like manner and posteriorly distinctly surpass the abdominal apex. So far, no synapomorphies of the two taxa from the first half of the Permian have been identified. The very short and transverse pronotum is likely an autapomorphy of †*C. archaica*. A thorough documentation of the structural features of early beetle fossils should have high priority. RTI is a very promising tool to obtain new and well-founded morphological data, which will allow a thorough phylogenetic evaluation of Permian beetles in future studies. We extended the conventional RTI workflow by focus merging and panoramic stitching, in order to overcome previous limitations. Taxonomic re-arrangements of stem group beetles including †*C. archaica* were suggested in recent studies by A.G. Kirejtshuk and co-workers. As they are not based on shared derived features they are irrelevant in a phylogenetic and evolutionary context.

Keywords

oldest beetle; Paleozoic; Lower Permian; fossil; stem group; imaging techniques

1. Introduction

1.1. The earliest beetles and their systematic treatment

Beetles form a very species-rich group comprising almost 400 000 described species (e.g. Zhang 2013). The clade Coleoptera has a very rich fossil record throughout the entire Mesozoic and Cenozoic (Wang et al. 2013). Its origin probably lies in the Carboniferous (e.g. McKenna et al. 2015, 2019; Zhang et al. 2018; Beutel et al. 2019), even though the oldest fossils do not appear earlier than in Permian sediments, leaving a considerable gap in the fossil record ('ghost lineage'). While remains of beetles – mostly consisting of isolated elytra – are frequent in the late Permian, only few records come from the early part of this geologic period (e.g., Ponomarenko 1995). By far most of the beetle fossils can be assigned to the crown group of Coleoptera (e.g., Crowson 1981; Ponomarenko 1995), but many Permian (and some Triassic) species belong to the (paraphyletic) stem group (e.g., Ponomarenko 1995; Beutel 1997; Beutel et al. 2008; 2019; Yan et al. 2017a). While the crown group of Coleoptera comprises the most recent common ancestor (=MRCA) of all extant beetles and all its descendants, including extinct forms, the stem group includes only extinct taxa that split off along the stem lineage between the MRCA of Coleoptera and Strepsiptera (Misof et al. 2014) and the MRCA of all living beetles. Many of the very old stem group fossils have traditionally been assigned to Archostemata – a group that also comprises slightly more the 30 extant species – due to their apparent similarity (e.g., Ponomarenko 1969; Kirejtshuk 2020). However, the morphological features shared by archostematan and Permian beetles are exclusively symplesiomorphies (Beutel 1997; Beutel et al. 2008, 2019). Morphology based phylogenies favour Archostemata as the sistergroup to all other extant beetles (e.g., Beutel et al. 2019; but see Lawrence et al. 2011), whereas recent phylogenetic studies based on molecular data support a sister group relationship with Myxophaga (McKenna et al. 2015, 2019; Zhang et al. 2018) and therefore a position nested within the crown group of Coleoptera.

†*Coleopsis archaica* Kirejtshuk, Poschmann and Nel, 2014 has been described as the oldest known fossil beetle in a study with a main focus on the elytral venation of the extinct group †Tshekardocoleidae (Kirejtshuk et al. 2014). The species has been described from a single specimen and since then no further material has been reported. The holotype comes from an early Permian deposit in western Germany (see below for further details) and is estimated to be about 297 million years old (Kirejtshuk et al. 2014). Initially, †*C. archaica* has been interpreted as a representative of †Tshekardocoleidae, based on similarities between the holotype and fossil remains attributed to this extinct group, and both were considered as members of Archostemata (Kirejtshuk et al. 2014). Later, it has been argued by the same first author that †*C. archaica* should not be placed within †Tshekardocoleidae but as a sister taxon to this group (Kirejtshuk and Nel 2016), or

alternatively as a sister taxon of a group that comprises †Tshekardocoleidae and †*Labradorocoleus carpenteri* Ponomarenko, 1969 (Kirejtshuk 2020). In both cases it was assumed that †*C. archaica* and †Tshekardocoleidae are located within a broad (and paraphyletic) concept of Archostemata (see Beutel 1997; Beutel et al. 2008, 2019). In a very recent study, Cai et al. (2022) assigned †*C. archaica* to a taxonomic unit Alphacoleoptera Engel, Cai, and Tihelka 2022 (= †Protocoleoptera Tillyard 1924 sensu Crowson 1981). They refer to this grouping as the “basalmost and extinct suborder of beetles” (Cai et al. 2022, Supplementary Information p. 11). The phylogenetic treatment of extinct groups in that study is not backed up by any arguments in a Hennigian sense (i.e., shared apomorphic features), and the fossils were not included in the phylogenetic analysis. Alphacoleoptera is apparently a paraphyletic assemblage (see e.g. Beutel et al. 2008, 2019; Yan et al. 2017b) that has been named in order to conform with the rest of the ranked nomenclatorial system used by Cai et al. (2022).

1.2. Reflectance Transformation Imaging

Reflectance transformation imaging (RTI) is a set of techniques used to capture images of the same field of view under different lighting conditions. The data are processed into a digital model of the photographed object that allows for virtual relighting. The virtual relighting is not limited to recreating the original lighting conditions, and it is possible to change various aspects of the model, such as removing surface colours and increasing the specularity of the surface. The RTI model also contains information on the topology of the imaged surface in form of surface normals (vectors that are perpendicular to the surface) for each pixel. Therefore, the RTI methods can, apart from virtual relighting, also be used to create 3D models (shape from shading) (Malzbender et al. 2006; MacDonald 2011).

In order to create an RTI model, images must be taken with a light source positioned differently for each individual image. The positions of the light sources have to be known in order to compute a model using the standard techniques (Malzbender et al. 2006). This can be achieved either by a geometrically exact placement of the light (usually arranged in a hemispherical dome), or alternatively by calculating the directions by photographing hemispherical objects with a high specularity and computing the light directions based on the reflections of the hemisphere (Mudge et al. 2006). The latter technique allows for a more flexible workflow and easier construction of dome-type setups (Kinsman 2016).

RTI has been widely adopted in various subfields of archaeology (Kotoula and Kyranoudi 2013; Newman 2015; Selmo et al. 2017) and art history (Hughes-Hallett et al. 2021). In palaeontology RTI provides a valuable alternative to competing techniques such as μ CT scanning or structure from motion techniques, such as photogrammetry or 3D laser scanning, especially for fossils with a

low relief that are located on flat surfaces (Hammer et al. 2002; Jäger et al. 2018; Kenchington et al. 2018). In palaeoentomology RTI turned out as a suitable method for imaging strongly compressed fossils, especially insect wings (Béthoux et al. 2016, 2021; Cui et al. 2018). While it is possible to produce RTI models of very small objects, the constraints of macro-photography regarding the depth of field and the field of view limit the application of a conventional RTI procedure (Cosentino 2013; Hughes-Hallett et al. 2021). Specialised workflows for overcoming the limited field of view through panoramic stitching (Kim et al. 2016; Aure et al. 2017), and for solving the problem of the narrow depth of field through focus merging (Lewis et al. 2021) have already been presented. However, they have not been applied to fossils of insects so far.

Even though †*C. archaica* was previously documented with drawings, photographs and SEM micrographs, the description is very short and apparently not fully compatible with the single known specimen. The obvious key role of †*Coleopsis archaica* in the phylogeny and early evolution of Coleoptera, and the availability of the Reflectance Transformation Imaging (RTI) as an alternative, complementary imaging technique induced us to re-examine the holotype. We demonstrate a fast and automated workflow to capture and process RTI images at a very small scale, with the option to extend the narrow field of view that results from high magnification through panoramic stitching, and also to recognize surface structures that are located on uneven surfaces of distinctly compressed insect fossils by recording and processing focus stacks.

While there is a relative abundance of fossils from the Permian that can be attributed to Coleoptera (including its stem group) (e.g. Ponomarenko 1969, 1995, 2000, 2016), the holotype of †*C. archaica* is the oldest specimen that can unambiguously be identified as a beetle. In contrast to many other fossils of similar age, not only the elytra are preserved. Therefore, this specimen is not only interesting regarding its age, but also highly relevant for future phylogenetic analyses that can shed light on the earliest evolution of beetles.

2. Material and methods

2.1. Material

This study is centred around a single fossil specimen, preserved as a thin layer of organic substance on two slabs of rock (part and counterpart). The specimen with the collection number ZfB 3315 is housed at the Geowissenschaftliche Sammlungen des Saarlandes, Referat D/2, Arten- und Biotopschutz, Zentrum für Biodokumentation in Schiffweiler, Germany.

The specimen originates from a small outcrop near the village Grügelborn near the town St. Wedel in the municipality of Freisen (Saarland, Germany) (Poschmann and Schindler 2004).

The rocks containing the fossil belong to the Humbert bed (silty claystones), located in the uppermost part of the Meisenheim Formation (Odernheim Unit, M10 = L-O10), which itself is part of the Rotliegend lithostratigraphic unit (Poschmann and Schindler 2004; Brauckmann 2007). The sediments from which the studied fossil originates are interpreted as lake sediments that were deposited within the Saar-Nahe Basin and underwent a light form of contact metamorphism (Poschmann and Schindler 2004; Brauckmann 2007). Slightly older sediments (also part of the Meisenheim Formation) have been dated to an age of 297.0 ± 3.2 million years based on uranium-lead dating of zircon crystals in volcanic tuff (Königer et al. 2002). This suggests a late Asselian or earliest Sakmarian age for the fossil (Kirejtshuk et al. 2014).

2.2. Imaging

The specimen was photographed using a Keyence VHX 7000 digital microscope with inbuilt focus merging and panoramic stitching functionality using coaxial white light with a cross-polarising filter setup. In some cases, multiple images of the same view with different exposure time settings were recorded for later processing.

In a different setup, images with different illumination directions (see next section) were recorded using a Nikon D7200 DSLR camera in combination with a Laowa 25 mm, f/2.8, 2.5–5× magnification objective. The specimen was placed on the microscopy table of a modified (upper part removed) Zeiss Standard microscope to position the object along the x, y and z axes. Images were taken of both rock slabs with different fields of view and different object distances. This was done without moving the microscopy table relative to the camera (except for the manipulation in the z-dimension) or the specimen relative to the microscopy table.

2.3. RTI dome

For reflectance transformation imaging (RTI) a dome-type setup (e.g., Kinsman 2016) was used to quickly change between illumination directions of point light sources. The setup consists of an array of 24 Nichia NVSW219CT 2W power LEDs with a luminous flux of 280lm and a colour temperature of 5000K that are mounted on the outside of a dark half-spherical plastic bowl with an inner diameter of ca. 220 mm, with circular holes allowing the light to pass through the dome. The LEDs were powered using a 12V 1A DC power supply and a MEAN WELL 9–36 V, 700 mA DC/DC power supply module. The power for the LEDs as well as the camera trigger cable was controlled using a 12V relay module with 16 relays and optocouplers. The relay module was controlled using an Elegoo MEGA 2560 R3 microcontroller.

A metal ball of a ballpoint pen, positioned on a piece of Fimo polymer clay (STAEDTLER Mars GmbH & Co. KG), served as a reference sphere to capture the light directions inside the RTI dome in the field of view of the

camera at the focal plane of the lens (see also Cosentino 2013; Béthoux et al. 2016). The Arduino integrated development environment (Arduino®, AGPL v. 3 license) was used to send commands from a computer to the microcontroller, to start a sequence of different illuminations and image captures.

2.4. RTI processing

For processing the captured images of the RTI setup, we used ‘relight’ (Ponchio et al. 2019) (available at <https://github.com/cnr-isti-vclab/relight>, accessed 12th of May 2022, GPL v. 3 license). The software was compiled on a Debian based Linux system, following the instructions provided in the software repository. The graphical user interface ‘relight’ was used to process the images of the reference sphere to create a light points (.lp) file, which shows the positions of the lights relative to the sphere as vectors in 3D space. This file was then used to process the images of the fossil using the command line program ‘relight-cli’ which was called from a Bash (GPL v. 3 license) shell script. From the results of the RTI processing only the normal maps – image files in which the directions of the normal vectors of a surface are stored as RGB colours – were used for further processing.

2.5. Image processing

Images of the same field of view were aligned using the command line program ‘align_image_stack’ of the Hugin software suite (GPL v. 2 license). The aligned images were then merged into in-focus images (extended depth of field) using ‘enfuse’ (GPL v. 2 license). The former two processes were also automated using a Bash script. Panoramic (stitched) normal map images of the fossil were created manually using GIMP (GPL v.3.0 license). The normal maps were converted into height maps – image files in which the (relative) height of points on a surface are coded as grey values – using the program AwesomeBump (GPL v. 3 license) on a Debian based Linux system with an Nvidia Quadro K4000 graphics card. In some cases (unrelated to the RTI processing), images of the same field of view with different exposure settings were merged (HDR, high dynamic range) using ‘enfuse’.

2.6. Graphic design

GIMP was used to optimise the images for colour, brightness, and contrast and to merge images of part and counterpart of the fossil by mirroring one image and placing it on top of the other as a separate layer with 50% transparency. Inkscape (GPL v.3.0 license) was used to produce the drawings and to arrange the figure plates. The circular graphic legends for the normal map and height map images (depicting the reference sphere) were made following (Béthoux et al. 2021; Cui et al. 2022).

2.7. Data availability

All herein used digital microscopy images are available from the Zenodo data repository at <https://doi.org/10.5281/zenodo.6550817>. Information regarding the construction and use of the RTI dome setup, all images captured with the RTI setup, as well as short instructions and scripts for processing the generated image data are available at <https://doi.org/10.5281/zenodo.6550889>.

3. Results

Coleopteroidea Handlirsch, 1903 (= Coleopterida)

Coleoptera Linnaeus, 1758

Coleopsis Kirejtshuk, Poschmann and Nel, 2014 (monotypic)

<https://zoobank.org/20837C14-27C0-4FFE-867D-08F2BD-04CC96>

Coleopsis archaica Kirejtshuk, Poschmann and Nel, 2014

<https://zoobank.org/39489AC9-DD98-461E-A315-D32A-CAC93729>

?Coleoptera. ?Tshekardocoleidae Poschmann and Schindler 2004, p. 304, fig. 7

Tshekardocoleidae gen. et sp. indet. Brauckmann 2007, p. 191, fig. 17

Coleopsis archaica Kirejtshuk, Poschmann and Nel 2014 in Kirejtshuk, Poschmann, Prokop, Garrouste and Nel 2014, p. 6, figs. 1, 4

Coleopsis archaica Kirejtshuk and Nel 2016, p. 71, figs. 1–5

Coleopsis archaica Kirejtshuk 2020, p. 10, figs. 2 A–C

Holotype (the only specimen). ZfB 3315, Zentrum für Biodokumentation, Schiffweiler, Germany.

Redescription. *General features.* The slender beetle is 7.8 mm long (including mandibles and elytra) and reaches its maximum width of 2.5 mm slightly anterior to the posterior third of the body. The anterior part of the body with the prognathous head and the short and transverse prothorax is unusually short in relation to the remaining body (prothorax + abdomen), which comprises ca. 80% of the total length. The elongate elytra reach beyond the abdominal apex (Fig. 1). The dorsal surfaces of the head and the pronotum display a pattern of fine cuticular tubercles. — *Head capsule.* The head is distinctly prognathous, about as broad as long, with rounded postocular temples and a short and moderately constricted neck region (Fig. 2A). Vestiges of dorsal ecdysial lines, the frontal and coronal sutures, are not recognizable. The head



Figure 1. †*Coleopsis archaica*, holotype, ZfB 3315, microscopic images, coaxial cross-polarised light, multi exposure bracketing. **A** photograph of more complete side (part); **B** less complete side (counterpart) virtually projected onto the part (the counterpart is mirrored); **C** photograph of the counterpart. Abbreviations: **A**, Analis (anal vein); **abd**, abdomen; **ce**, compound eye; **CuA**, Cubitus anterior; **edt**, elytral distal tip; **elc**, elytral antero-proximal corner; **elf**, elytral flange; **elpm**, elytral posterior margin; **hw**, hind wing; **iv**, intercalary veins; **leg1**, foreleg; **pnlp**, lateral process of the pronotum; **pn**, pronotum.

capsule is slightly narrowing anterior to the compound eyes. Dorsal protuberances (see Beutel et al. 2008) are visible but rather inconspicuous (best visible in the black-and-white height maps; Fig. 2A, B). The compound eyes are large and strongly convex, strongly protruding laterally. Ocelli are not present. Antennal insertions, tentorial pits, maxillary grooves, and gular sutures are not visible. — *Labrum*. The labrum is well-developed, broad, with rounded anterolateral angles and lacking an anteromedian emargination. — *Antennae*. Not preserved. — *Mandibles*. The mandibles are moderately sized, exposed laterad the labrum, laterally evenly curved, and distinctly protruding beyond the anterior labral edge, with a single visible apical tooth. — *Maxillae*. The maxillary body is likely visible on the right side, posterolaterad the labrum (Fig. 2A, 3A). A part of the maxillary palp is recognizable on both sides. — *Labium*. A large plate-like structure, likely comprising the mentum and prementum, is visible. It has

a laterally rounded anterior margin and a seemingly very distinct, straight hind margin (possibly congruent with the anterior margin of the frons). An indistinct, straight transverse suture is present on the anterior third. The labial palps and endite lobes are not visible. — *Prothorax*. The transverse pronotum is more than three times as wide as its length along the midline. It is very slightly convex anteromedially and nearly straight posteriorly. Laterally it is strongly explanate, forming thin lateral duplicatures with a coarsely serrated margin. The anterolateral edges are distinctly projecting anteriorly. Posterolateral angles are indistinct or absent. The outlines of the small, rounded and medially separated procoxae are recognizable. A broad postcoxal bridge is obviously missing, suggesting posteriorly open procoxal cavities. The parallel-sided profemora are visible between the posterior pronotal margin and the concave anterolateral elytral edge. Other distal parts of the legs (e.g. pro-, meso- or metatibiae)

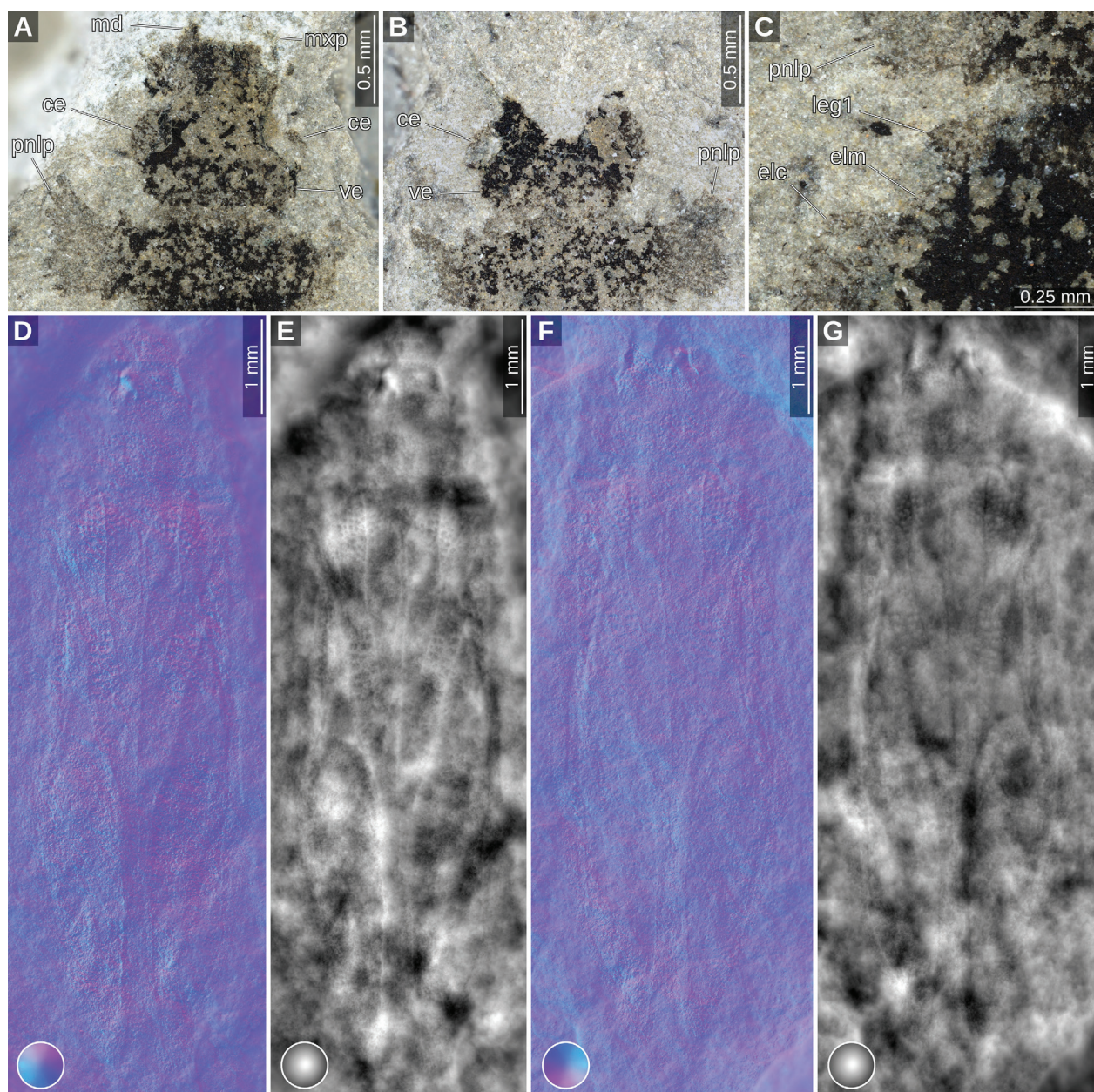


Figure 2. †*Coleopsis archaica*, holotype, ZfB 3315. **A–C** microscopic images, coaxial cross-polarised light, multi exposure bracketing. **A** detail of the head and prothorax region, part; **B** detail of the head and prothorax region, counterpart; **C**: detail of the left side of the mesothoracic region, part; **D–G** images derived from RTI imaging, the circular legends in the lower-left corners depict the convex half sphere used to calibrate the RTI setup under the same conditions as the images; **D** normal map representation of the part; **E** relative heights representation of the part; **F** normal map representation of the counterpart. Abbreviations: **G** relative heights representation of the counterpart. **ce**, compound eye; **elm**, elytral margin; **elc**, elytral antero-proximal corner; **leg1**, foreleg; **md**, mandible; **mxp**, maxillary palp; **pnlp**, lateral process of the pronotum; **ve**, venter.

(depicted in Kirejtshuk et al. 2014, fig. 1) are not recognizable. — *Mesothorax*. The large and exposed triangular scutellar shield is about as long as the pronotum. Ovoid and slightly oblique mesocoxae are indistinctly visible, slightly separated medially. Other parts of the mesothorax except for the elytra are not recognizable. — *Elytra*. The elytra are long and slender, comprising about 80% of the total body length, and nearly 5x as long as their maximum width. The shoulder region is distinctly retracted, almost to the level of the posterior edge of the scutellar shield, thus forming a distinct concavity of the anterior elytral edge. Broad explanate lateral flanges are present instead

of typical inward folded epipleurae. They apparently cover the posterior body in a loose tent-like manner without forming a tightly sealed subelytral space. Posteriorly they distinctly reach beyond the abdominal apex. Several distinct longitudinal veins with a non-parallel-arrangement are present, comprising C along the lateral edge, a rather indistinct Sc which almost reaches the elytral apex, an equally long and distinct vein (either representing R or R+MA), a long CuA which traverses the elytra from the anterolateral region (almost at the anterior edge of R) almost to the elytral tip, and a single anal vein (A) about 1/3 as long as the elytron. All longitudinal veins

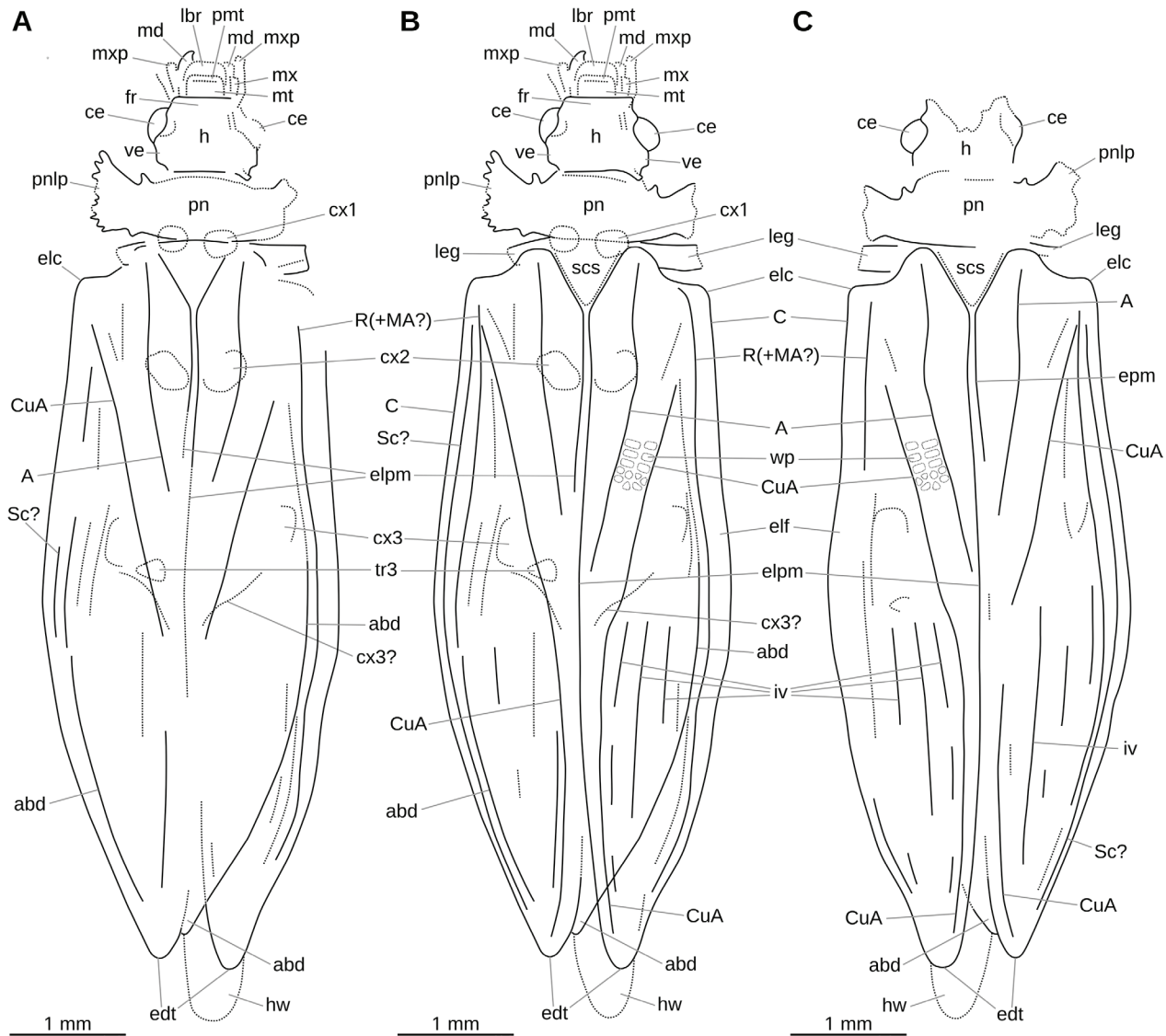


Figure 3. †*Coleopsis archaica*, holotype, ZfB 3315, drawings based on the photographs and the RTI images. **A** more complete side (part); **B** part and counterpart combined (counterpart mirrored); **C** counterpart. Abbreviations: **A**, Analis, anal vein; **abd**, abdomen; **C**, Costa; **ce**, compound eye; **CuA**, Cubitus anterior; **cx1–3**, coxa of thoracic segments 1–3; **edt**, elytral distal tip; **elc**, elytral antero-proximal corner; **elf**, elytral flange; **elpm**, elytral posterior margin; **fr**, frons; **h**, head; **hw**, hindwing; **iv**, intercalary veins; **lbr**, labrum; **leg1**, foreleg; **md**, mandible; **mt**, mentum; **mx**, maxilla; **mxp**, maxillary palps; **pmt**, prementum; **pn**, pronotum; **pnlp**, lateral process of the pronotum; **R(+MA?)**, Radius, possibly conjoined with Media anterior; **Sc**, Subcosta; **scs**, scutellar shield; **tr3**, metatrochanter; **ve**, venter; **wp**, window punctures, exemplary, not limited to this area of the wing.

are unbranched. Several shorter and rather indistinct longitudinal veins with unclear homology are present on the posterior 1/3, designated tentatively here as intercalary veins (secondary [or supplementary] longitudinal veins). Cross veins are missing. Window punctures are recognizable between CuA and A on the anterior 1/3 of the elytra but indistinct, arguably an artefact caused by the strong compression of the fossil. — *Metathorax*. The indistinctly visible meso- and metacoxae indicate that the metathorax is slightly longer than the mesothorax, but the border between both segments is not recognizable. The metathorax appears almost parallel-sided, only slightly widening posteriorly as suggested by the position and outline of the coxae. The anapleural suture and the pleural elements are not recognizable, and a median discrimin, a transverse ridge and an exposed metatrochantin are also not visible.

The indistinctly recognizable metacoxae are transverse. An indistinct oblique line, likely the posterolateral edge, tentatively suggests that the mesal metacoxal portion was distinctly projecting into the anterior abdomen. Metacoxal plates are not recognizable and are probably missing. A triangular metatrochanter with rounded edges is visible. Distal parts of the hind legs are not preserved. — *Hind wings*. The rounded apical part of the membranous hind wings, clearly visible on the right body side (Fig. 1), distinctly projects beyond the elytral apex. The exposed apical wing portion does not show any trace of folding or rolling, and no veins are visible on this region. — *Abdomen*. The abdomen is evenly rounded laterally and tapering towards its sub-acuminate apex. It ends distinctly before the elytral apices. Individual sternites are not visible (in contrast to Kirejtshuk et al. 2014).

Updated species diagnosis. Body medium-sized (7.8 mm total length), slender. Head prognathous. Eyes strongly protruding laterally. Prothorax short. Pronotum more than three times as wide as its length along the midline, with anterolateral processes distinct, and lateral portions distinctly explanate with coarsely serrated margin. Procoxae small, rounded and medially separated. Dorsal surface of head and pronotum with fine tubercles. Scutellar shield triangular and large. Elytra reaching well beyond abdominal apex. Elytral shoulder region emarginated, with distinct concavity. Elytra with broad explanate lateral flanges. CuA oblique, from anterolateral region almost to the elytral tip; single anal vein (A) about 1/3 as long as the elytron. Window punctures visible between CuA and A. Mesocoxae ovoid and slightly oblique. Metathorax slightly longer than mesothorax.

This diagnosis is explicitly stated as a species-level diagnosis. Since †*Coleopsis* is monotypic, as are †Coleopseidae (and †Coleopseoidea Kirejtshuk and Nel 2016), the diagnosis should only be used to distinguish further specimens from †*C. archaica*. It should not be arbitrarily split up into parts which then could lead future authors to include additional species into the (presently) monotypic taxonomic category, without providing an apomorphy-based argumentation or a phylogenetic analysis.

4. Discussion

The ‘peril of dating beetles’ has been pointed out by Tous-saint et al. (2017), and the risk of placing fossils without proper phylogenetic evaluation was demonstrated in a comprehensive case study on †*Leehermania prorova* Chatzimanolis, Grimaldi and Engel 2012 (Fikáček et al. 2020). Another source of problems in the context of fossils of beetles and other groups of organisms is insufficient documentation and description of morphological features. As shown for instance in the case of an alleged Devonian nymph of a pterygote insect, †*Strudiella devonica* (Garrouste et al. 2012), this can lead to serious phylogenetic misinterpretations (Hörnschemeyer et al. 2013). This applies to fossils in general, but especially to phylogenetically crucial species. One such case is doubtlessly †*Coleopsis archaica*, correctly identified as the oldest presently known beetle by Kirejtshuk et al. (2014).

4.1 New interpretation of morphological features

†*Coleopsis archaica* has been described and illustrated in Kirejtshuk et al. (2014). Our re-evaluation of the single known specimen (holotype) revealed distinct discrepancies with this earlier interpretation. Despite considerable differences between our interpretation of the mouthparts and the drawings in Kirejtshuk et al. (2014, fig. 1A–B), we confirm that the labrum is not fused with the head

capsule and appears to be movable. From the palps of the maxilla and the labium, which are described in Kirejtshuk et al. (2014), we could only identify those of the maxilla, without recognizable individual palpomeres. Similarly, we did not find a transverse ridge on the posterodorsal head region as depicted by Kirejtshuk et al. (2014). It is very likely a structure of the ventral side.

We confirm an unusually short and transverse pronotum, as shown in Kirejtshuk et al. (2014). However, in contrast to the illustrations in that study, at least a moderately distinct posterolateral angle is recognizable and the lateral parts of the pronotum are strongly explanate and have a coarsely serrated margin. The prosternum was illustrated and described as visible on one of the slabs and claimed to be as long as the pronotum (Kirejtshuk et al. 2014). In contrast, we found that it is not visible on either of the slabs. Both mostly show features of the dorsal surface, and some pressed-through features of the ventral side.

The illustrations in the original description (Kirejtshuk et al. 2014, fig. 1B) as well as our observations and interpretation (Fig. 3A, B) suggest that the prosternal process is very small or absent, and that a posterior procoxal closure (e.g., Ponomarenko 1969) is missing. We can confirm the presence of the profemur in the studied fossil, but we could not locate a protibia as depicted in Kirejtshuk et al. (2014, fig. 1A, B).

We found the mesoscutellar shield (‘scutellum’) to be much larger than shown in the illustrations of Kirejtshuk et al. (2014, fig. 1A), which is congruent with the comparative discussion in Kirejtshuk and Nel (2016), but not with the description and the diagnosis in the former work. From a mesothoracic leg we could only identify the mesocoxa, which is of about the same shape and size as depicted in Kirejtshuk et al. (2014, fig. 1B). The mesofemur and mesotibia, which are described in Kirejtshuk et al. (2014), are not visible in the fossil.

Kirejtshuk et al. (2014, p. 581) described the elytra as “wider than prothorax, sides apparently subexplanate”. Even though the term “subexplanate” is vague, this appears to conform with our interpretation that broadly explanate lateral elytral flanges were present, instead of elytral epipleura folded inwards and forming a closed subelytral space. Kirejtshuk et al. (2014) described the shoulders of the elytra as ‘moderately raised’. While the elytral shoulders are indeed raised, this description does not fully acknowledge the shape of the elytral margin in the shoulder region, which even contains a short concave section (Figs 2C, 3). This was not depicted in the original drawings (Kirejtshuk et al. 2014, fig. 1A, C). We found the venation of the elytra very difficult to interpret due to the preservation of the specimen. The veins are recognizable as dotted lines of dark organic matter (or the absence of such on the counterpart; Fig. 1A, C) and as faint longitudinal impressions on the surface of the fossil (Fig. 2D–G). In some elytral areas the distinction between veins and the margin of the thorax and the abdomen is challenging (e.g., in Fig. 3A the vein R(+MA?) and the lateral margin of the abdomen). The veins that lie between what

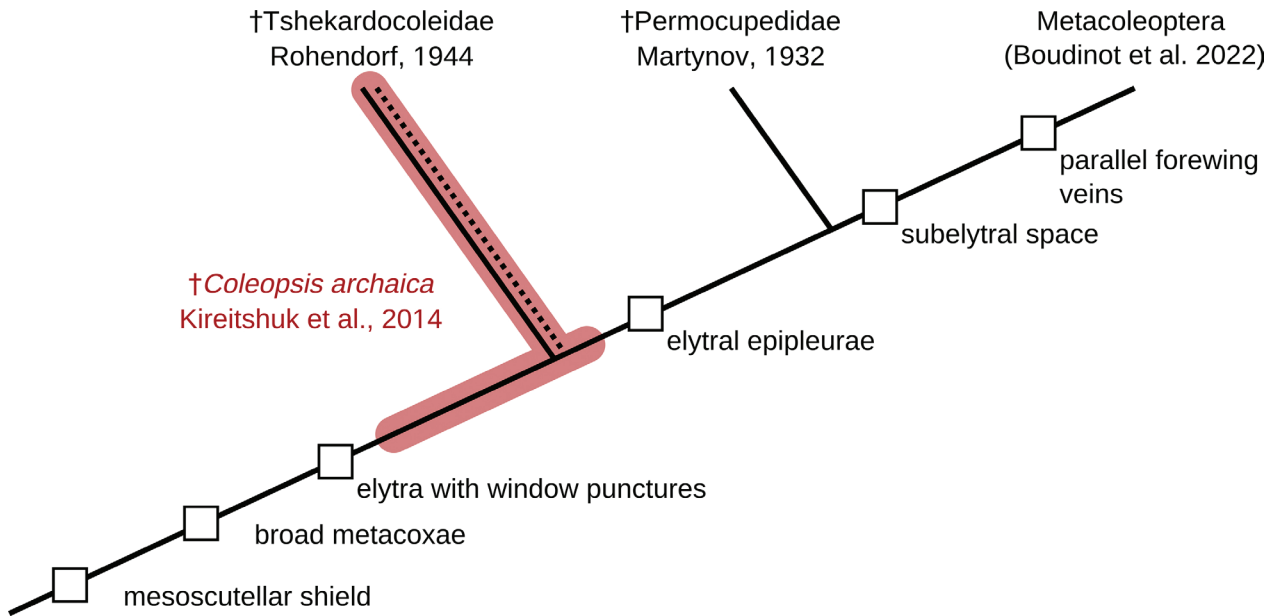


Figure 4. Phylogenetic position of *†Coleopsis archaica* (red) based on apomorphies visible in the fossil re-described here. *†Tshekardocoleidae* is designated as potentially non-monophyletic, due to the absence of apomorphic characters. The clade Metacoleoptera (Boudinot et al. 2022) includes all extant beetles and the stem group taxa except for *†Tshekardocoleidae*, *†Permocupedidae* and *†Coleopsis archaica*.

we interpreted as radius (possibly conjoined with media anterior) and cubitus anterior, were interpreted by Kirejtshuk et al. (2014) as radius posterior 1 and 2 (RP₁ and RP₂) and as the media (M). In Kirejtshuk et al. (2014, fig. 1A, C), they are depicted as originating from the two above-mentioned veins (our R(+MA?) and CuA). However, while we also found three veins to be present in this area, we could not trace the origin of the three of them. We therefore tentatively interpret them as intercalary veins. Posterior to the CuA vein we could find a structure that could be interpreted as CuP (cf. Kirejtshuk et al. 2014, fig. 1A). However, we are unsure whether this structure represents a vein, and we could also not see a conjunction of it with the anal vein as described and depicted in Kirejtshuk et al. (2014, fig. 1A). It is also noteworthy that this is displayed very differently in another figure of the same publication (Kirejtshuk et al. 2014, fig. 1C, left side of the drawing). A second anal vein (A₂) is apparently absent in the studied fossil. Judging from the supposed position of this vein, it appears likely that a mesocoxal structure has been mistakenly interpreted as a vein by the authors of the original description.

In contrast to the drawing accompanying the original description (Kirejtshuk et al. 2014, fig. 1B), we did not identify the metathoracic katapisternum and the transverse suture of the metaventrite as recognizable structures. The metacoxae are apparently transverse as shown in Kirejtshuk et al. (2014, fig. 1B), but only faintly impressed. In contrast to the drawing in Kirejtshuk et al. (2014, fig. 1C), we could not find remains of the metafe-mur and of the metatibia. Kirejtshuk et al. (2014, fig. 1B) depicted the abdomen with five distinct sternites. In clear contrast to this, we could not see any traces of individual abdominal sternites in the fossil specimen.

4.2. Systematic interpretation

Whereas the position of *†Coleopsis archaica* in Coleoptera in the widest sense is beyond reasonable doubt, the old age together with its suggested basal position in the phylogenetic tree of beetles (Kirejtshuk and Nel 2016; Kirejtshuk 2020), make it necessary to carefully discuss the documented characters of the fossil. The name Coleoptera (greek koleos = sheath) indicates an easily visible autapomorphy of the group, fore wings transformed into shell-like sclerotized elytra. However, aside from this, the megadiverse clade has not been commonly associated with a single apomorphic character state, probably because extant beetles share a rich set of derived features that very clearly separate them from species of any other insect lineages (e.g., Ponomarenko 2005; Lawrence et al. 2011; Beutel et al. 2019). It is apparent that a careful assessment of documented structural features of fossils is necessary to enable their robust interpretation as members of the stem group or crown group (i.e. the smallest group that comprises all extant representatives).

4.3. Coleopteran autapomorphic character states documented in the fossil (features shared with other extinct and extant beetles)

As pointed out above hardened protective forewings (elytra) are one of the most distinctive features of beetles and have likely played a crucial role in the earliest evolutionary history of the group. In the form in which they are present in extant beetles (epipleura, parallel stripes or smooth surface, various locking mechanisms, etc.), they

contain an entire set of apomorphic character states (e.g., Beutel and Haas 2000; Lawrence et al. 2011). However, the mere presence of heavily sclerotized forewings is not sufficient to identify a fossil specimen as a representative of Coleoptera. This was for instance shown in the case of †*Umenocoleus* Chen and T'an 1973, two species originally described as beetles (Chen and T'an 1973). Later, they were interpreted as dictyopterans (Vršanský 1998, 2003), then again assigned to Holometabola and Coleoptera by Kirejtshuk et al. (2014). Finally, together with a few other species, they were included in Umenocoleidae, as the sister group of Alienopteridae, and this clade was placed as the sister taxon of Mantodea (Beutel et al. 2020; Luo et al. 2022). An older case underlining the potential peril of misinterpreting sclerotized forewings is †*Protocoleus mitchelli* Tillyard, 1924, the namesake of Protocoleoptera (e.g. Crowson 1981), which was already recognized as an extinct species of Polyneoptera by Kukulová (1966).

Apart from well-sclerotized elytra, albeit lacking infolded epipleura, the holotype of †*Coleopsis archaica* displays other morphological features that allow for a robust attribution to Coleoptera including the stem group. The lack of exposed membranes is a key innovation and autapomorphy of Coleoptera (e.g., Beutel et al. 2008; McKenna et al. 2019), and this feature was very likely present in †*C. archaica* despite the imperfect preservation of the fossil. A distinctly prognathous and more or less wedge-shaped head, as it is clearly present in †*C. archaica* (Fig. 1), is another derived ground plan feature of Coleoptera. In contrast to Kirejtshuk et al. (2014), the abdominal segmental borders are not visible in the holotype. However, it appears likely that only 5 exposed ventrites are present like in the vast majority of extinct (e.g. Ponomarenko 1969; Yan et al. 2017b, 2017a) and extant groups (Lawrence et al. 2011), and that a more or less parabolic sternite VII was terminal. The retraction of the terminal abdominal segments would be an additional autapomorphy of beetles including the stem group.

A groundplan feature of Coleoptera in the widest sense is likely the presence of elytral window punctures (e.g., Beutel et al. 2008; Friedrich et al. 2009; Lawrence et al. 2011), a feature unknown in any other group of insects including †Umenocoleidae with their shell-like, hardened fore wings (Beutel et al. 2020; Luo et al. 2022). The condition in †*Coleopsis archaica*, window punctures present but only recognizable on a limited elytral region (Fig. 2D–G), appears ambiguous. One possible explanation is that the lack of window punctures in most elytral areas is a plesiomorphy retained by †*C. archaica*, compared to other stem-group beetles (Ponomarenko 1969; Beutel et al. 2008) and extant Cupedidae and Ommatidae (e.g. Friedrich et al. 2009; Lawrence et al. 2011). However, as the window punctures are likely remains of the original wing membrane, this interpretation is rather unlikely. Based on the presently available information we assume that the limited area with punctures is either an autapomorphy of the species or more likely just an artefact caused by the strong compression of the

holotype. Window punctures (and tubercles) were likely also present on other elytral regions, even though only very indistinctly visible and more or less impossible to visualize.

4.4. Plesiomorphic character states of the fossil (features not shared with extant beetles)

In extant beetles and stem group fossils with the notable exception of †Tshekardocoleidae (Boudinot et al. 2022), the elytra form a tight sheath around the dorsal and lateral posterior body, thus forming a tightly sealed subelytral space. This key innovation in early beetle evolution is clearly missing in †*C. archaica*. Even though the holotype is preserved as a strongly compressed fossil, it is apparent that the lateral elytral margins are not bent ventrad or even inwards (Fig. 1A), and that the elytral margin is not fitting with the lateral margin of the abdomen. The absence of elytral epipleurae and a tightly secluded subelytral space is an obvious symplesiomorphy shared with species of †Tshekardocoleidae (Boudinot et al. 2022). Additionally, elytral tips distinctly surpassing the abdominal apex is clearly a plesiomorphic feature maintained in tshekardocoleid fossils and in †*C. archaica*.

The middle Permian †Permocupedidae are still somewhat ambiguous with respect to this feature (Ponomarenko 1969; Beutel 1997; Beutel et al. 2008), but apparently a very tight fit of the elytra and posterior body is not reached yet (Boudinot et al. 2022). It is safe to say that all other Permian and younger groups including the coleopteran crown group share a hermetically closed subelytral space, with a close fit of the posterior thorax and abdomen with the laterally infolded elytral epipleura. This is likely a synapomorphy of a clade Metacoleoptera (Fig. 4; Boudinot et al. 2022), which comprises all beetles except for †Tshekardocoleidae and †Permocupedidae, and also †*Coleopsis archaica*.

Another obvious symplesiomorphy of †*Coleopsis archaica* and species of †Tshekardocoleidae is the elytral pattern. In very distinct contrast to a strictly parallel arrangement of longitudinal veins (or ridges) in groups of the Upper Permian (Ponomarenko 1969; Yan et al. 2017b) and in extant Cupedidae and Ommatidae (Friedrich et al. 2009), the visible longitudinal veins (Sc, R(+MA?), CuA and A) form an irregular pattern, and CuA traverses the elytral disc obliquely almost from the shoulder region to the mesal elytral apex.

A likely ground plan apomorphy of Coleoptera in the widest sense is the presence of a tuberculate surface of exposed sclerites, arguably linked with a preference for narrow spaces under bark (e.g., Beutel et al. 2008). Even though the tubercular pattern is quite indistinct in the holotype of †*Coleopsis archaica*, this is probably due to poor preservation, like in the case of the window puncture. In any case, the dorsal surface does not appear smooth as it is the case in many extant groups of beetles, and also in several extinct lineages such as for instance Ademosynidae (Yan et al. 2017a).

4.5. Possible affinities within Coleoptera

The species in the focus of this study, †*Coleopsis archaica*, has been assigned to the Lower Permian †Tshekardocoleidae based on the similarity to species attributed to this group (Kirejtshuk et al. 2014). Later it has been argued that †*C. archaica* is not nested within this extinct group but is closely related to it (Kirejtshuk and Nel 2016). More recent studies have argued for a less close relationship between †*C. archaica* and †Tshekardocoleidae (Kirejtshuk 2020; Cai et al. 2022). It is important to note that none of these systematic interpretations was based on an argumentation using synapomorphies. Instead, the conclusions, distinctly varying in subsequent studies, are largely based on pure similarity, an approach discarded in systematics since Hennig (1950).

Three of the studies that discuss the affinity of †*C. archaica* (Kirejtshuk et al. 2014; Kirejtshuk and Nel 2016; Kirejtshuk 2020) suggest a close relationship to extant archostematan species without providing a clear phylogenetic argumentation. Palaeozoic beetle fossils, and especially those with a prominent elytral window puncture pattern, have been associated with Archostemata in different publications (e.g. Ponomarenko 1969; Kirejtshuk 2020). However, the similarity between extant archostematan beetles and Palaeozoic beetle fossils is mainly (or entirely) based on plesiomorphic features retained in extant Cupedidae and Ommatidae and not on autapomorphies (e.g., Beutel et al. 2008, 2019; Boudinot et al. 2022).

Cai et al. (2022) included †*Coleopsis archaica* in an assemblage Alphacoleoptera Engel, Cai, and Tihelka 2022, which is used as a synonym for Protocoleoptera Tillyard 1924 (sensu Crowson 1981). It is argued that Protocoleoptera cannot be used inside Coleoptera, as the type species does not belong to this holometabolous clade. Cai et al. (2022, Supplementary Information p. 11) refer to Alphacoleoptera as the ‘basalmost and extinct suborder of beetles’. Together with the lack of apomorphies in the diagnosis (Cai et al. 2022, Supplementary Information p. 11) this clearly suggests that Alphacoleoptera is not a monophyletic group. Therefore, any discussion on whether †*C. archaica* should be included in Alphacoleoptera is of no phylogenetic relevance.

†Tshekardocoleidae is currently said to comprise 15 species, all of which are based on fossils from the Permian (Kirejtshuk 2020). A close inspection of the most recently published diagnosis of †Tshekardocoleidae (Kirejtshuk et al. 2014, p. 3) reveals that some of the characters need further confirmation (e.g. the presence of 13 antennomeres) and none of the diagnostic character states represents a clear autapomorphy of the group. All of the character states are either clearly plesiomorphic (e.g. the presence of transverse metacoxae and 5 movable abdominal ventrites) or with an unclear polarity (e.g. pronotum with (sub-)explanate sides). This raises doubt about the monophyly of †Tshekardocoleidae. With respect to the systematic interpretation of †*C. archaica*, the question whether it is located within that group cannot be ad-

ressed as long as †Tshekardocoleidae lack apomorphies and thus support as a clade (Fig. 4). Support for a closer relationship with any species of †Tshekardocoleidae is also missing.

Considering the possibility that †Tshekardocoleidae is not a monophyletic group, careful comparisons of individual fossils are crucial to reveal relationships between species and genera, to be able to create a stable (apomorphy-based) taxonomy and to increase our understanding of the early evolution of beetles. Kirejtshuk et al. (2014) already attempted to compare †*C. archaica* and species attributed to †Tshekardocoleidae in some detail. However, we found that some of the described differences are flawed by misinterpretation. The length of the hind wings, for instance, and also the size of the mesoscutellar shield of †*C. archaica* were clearly underestimated (see above). Additionally, structures were illustrated that are definitely not recognizable, for instance, borders between abdominal sternites. Moreover, the drawings supposedly showing a dorsal and a ventral aspect of the holotype are not fully compatible. Boudinot et al. (2022) revealed distinct misinterpretations in descriptions (and drawings) of species attributed to †Tshekardocoleidae, for instance in the elytral venation of †*Sylvacoleus richteri* (cf. Boudinot et al. 2022, fig. 6B vs. Ponomarenko 1963, fig. 3A). With high-quality photographs only being available for some of the species, the amount of ambiguous interpretations in the original descriptions is difficult to estimate. It is apparent that new high-quality data have to be procured through investigation of the fossil specimens in order to allow for a reliable phylogenetic interpretation and the suggestion of a stable classification.

Few features of †*Coleopsis archaica* are potential autapomorphies. These include the exceptionally short and transverse pronotum and the presence of a fringe of setae or spines along the lateral elytral edge. However, the latter feature may arguably belong to the ground plan of Coleoptera in the widest sense, since more or less frayed or spinose pronotal or elytral fringes have also been described in different Cretaceous species of Ommatidae (e.g. Li et al. 2020).

4.6. RTI technique

Reflectance Transformation Imaging is widely used in cultural heritage research (e.g. Kotoula and Kyranoudi 2013; Boute et al. 2018; Hughes-Hallett et al. 2021). Despite its suitability for palaeontological applications, the adoption by palaeontologists, especially in the field of paleoentomology (e.g. Béthoux et al. 2016), has remained limited to a small circle of researchers. RTI techniques are especially useful to visualise small-scale surface details on otherwise flat surfaces, due to the high spatial resolution that can be gained compared to other methods such as 3D laser scanning or photogrammetry (MacDonald 2011; Porter et al. 2016). This makes it an ideal tool to study strongly compressed fossils or fossils with fossils with overall flat surface portions with a shallow relief, such as fossils of insect wings, where the additional

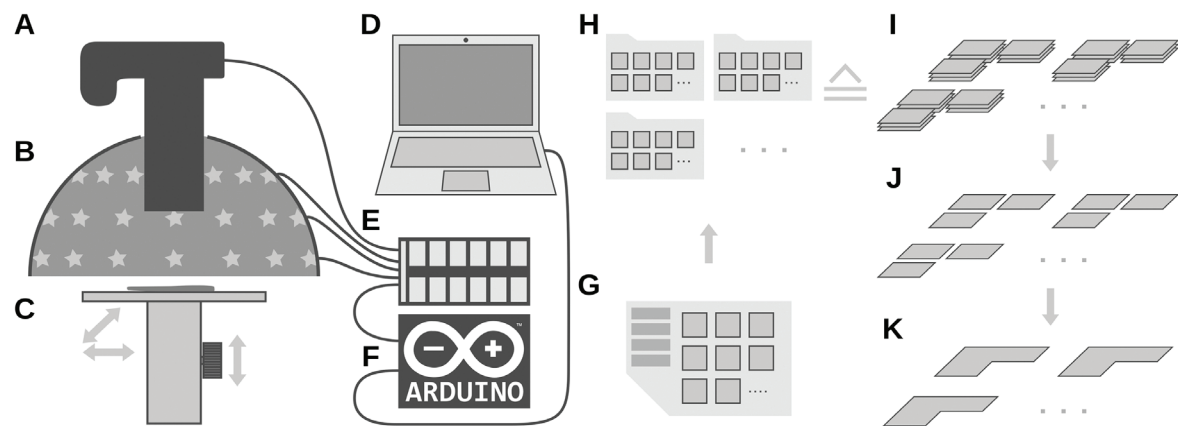


Figure 5. Schematic depiction of the RTI workflow used herein and the included hardware components (A–G). **A** Digital camera with a macro objective mounted on a vertical macro stand; **B** Half-spherical dome with power LEDs mounted with the light directed towards the centre of the dome; **C** XYZ-stage on which the fossil is placed; **D** Computer with Arduino integrated development environment (used for communication with the microcontroller and to trigger the camera shutter); **E** Relay board used to open and close specific parts of the circuit that powers the LEDs; **F** Arduino microcontroller used to control the relay board; **G** Memory card inserted into the camera used to save images and to transfer them to the computer; **H–K** Digital workflow used to create in-focus panoramic images; **H** Sorting the images from the camera into folders that each contain one RTI sequence (in our case 24 images corresponding to 24 illumination angles), in order to be automatically processed by the RTI software (relight); **I–K** Operations performed on normal maps, produced by the RTI software; **I** Normal maps with the same field of view but with different focal plane heights form ‘focus stacks’; **J** In-focus normal maps created by merging the images of each focus stack (extended depth of field); **K** Panoramic images created by stitching together images of the same objects with different fields of view. These can then be converted from normal maps to height maps.

information gained by RTI can help to understand the venation pattern (e.g., Demers-Potvin et al. 2020). Visualising wing venation in strongly compressed fossils can be considered one of the sweet spots of RTI, as the veins are often only represented by relief with very shallow but distinct elevations, which renders them poorly visible under diffuse light conditions. In addition, the veins often extend in different directions, which makes it necessary to use multiple grazing-light images rendering all veins visible as shadows. Compared to other techniques that are suitable for capturing very fine surface details, such as 3D surface scanning and micro-computer-tomography, RTI can be a much less cost intensive alternative.

The adoption of RTI in the field of paleoentomology is still very limited despite of its apparent potential. Several factors could have impeded a more widespread adoption. While hardware for constructing an RTI setup can be purchased for a modest price (ca. 120 € without shipping fees for our dome setup), the cost of a commercial prebuilt solution can be much higher (e.g. Bron Elektronik AG, <https://bronzcolor.swiss/de/produkte/scope-d50>, accessed April 11th 2022, ca. 23600 €) and the available setups might not be optimised for imaging very small objects. Even though constructing an RTI dome setup requires only beginner-level skills in electronics and microcontroller programming (Kinsman 2016), this still might represent a hurdle that stops potential users from adopting an RTI workflow. Another limiting factor is the availability of software. The predominantly used software RTIBuilder (Universidade do Minho and CHI, https://culturalheritageimaging.org/What_We_Offer/Downloads/Process/, accessed 12th of May 2022, GPL v. 3 license) has not been updated for a long time and is only available for

MacOS and 32 bit versions of Windows, limiting the choice of computer hardware that can be used to process multi-lighting images into RTI models.

For processing our RTI data we used ‘relight’ (Ponchio et al. 2019, <https://pc-ponchio.isti.cnr.it/relight>), which is another free program (GPL v. 3 license) that allows creating RTI models from multi-lighting image sets and offers both a graphical as well as a command-line interface. Using the command-line version, it is possible to invoke the program in scripts and create an automated workflow that requires little repetitive work. However, ‘relight’ is presently only available as source code and requires compiling the program to use it. This also could hamper the increased application of RTI technology.

Photographing very small details of fossils (e.g., insects) comes with two challenges. The small scale of the objects requires a high magnification, which in turn limits the area that can be recorded in a single image (narrow field of view). Further, the high magnification leads to a shallow depth of field. These challenges can be overcome by combining single images into a larger panoramic view by using ‘stitching’, and by combining the in-focus areas of multiple images of the same view to an overall in-focus image by using ‘extended depth of field’/‘focus merging’. Naturally, these two challenging factors also apply to images taken with an RTI setup. Solutions to overcome the limitations of a narrow field of view by creating panoramic images (Kim et al. 2016; Aure et al. 2017), and the limitations regarding the depth of field by focus-merging (Lewis et al. 2021) have already been demonstrated separately. However, to our knowledge have never been applied to RTI data of fossils.

As the surface shape was the centre of our interest, and for convenience, we did the focus merging and the panoramic stitching on the normal maps (surface topology). However, it should also be possible to apply these steps to image-based representations of colour and reflective properties. These can be generated with ‘relight’ (Ponchio et al. 2019), to create relightable scenes (complete RTI models). Panoramic stitching and focus merging of RTI data work only if the object, the camera, and the lights are not rotated or tilted between the captures. Otherwise one would have to correct for the effect, which would require knowing the exact parameters of the distortion. Therefore, translating the fossil (or the entire camera setup) should be done using a dedicated device like a microscopy table. As with regular images recorded as a focus stack (same field of view and a variable height of the focal plane), also normal maps that form a focus stack can be merged into a single, in-focus image. This is possible because the normal maps also contain blurry, out-of-focus areas that can be recognised by focus merging programs. Focus merging could also be done using the original images and not the normal maps. The latter could then be created from the in-focus (already merged) images. However, aside from being more complicated regarding the file handling, using the conventional workflow would result in the RTI model suffering from indeterminable light directions. Due to the z-axis movement, the light directed towards the centre of the focus-merged image could not be described by a single vector, potentially leading to artefacts (the larger the z-axis movement, the larger the artefact).

Normal maps can not only be used as part of a relightable RTI model, but also as a graphical representation of a fossil to aid the interpretation of surface details (e.g., Béthoux et al. 2021, Fig. 2D, F). However, with more complicated textures it can be difficult to intuitively interpret the surface shape. Since normal maps contain information about the orientation of each point on a surface, they can be converted into 3D models, which can then either be displayed as a video sequence or an interactive scene. Additionally, it is possible to store the 3D information in a 2D greyscale image where the grey values represent the elevation (‘depth map’). Depth maps can be used as a graphical representation of surface shapes (Fig. 2E, G), and can serve as a complementary, more intuitively interpretable way of presenting 3D surface shapes in 2D figures.

While the depth maps used in this study show a good spatial resolution (Fig. 2E, G), they strongly differ from depth maps produced by a digital microscope, which probably (proprietary closed source software) calculates the elevation using a ‘shape from defocus’ approach. The deviations can be explained by artefacts introduced with the focus merging and panoramic stitching as well as by the conversion from normal maps to depth maps. The depth maps produced by our workflow should therefore be seen as maps of relative heights rather than exact three-dimensional representations of the fossil. To combine high spatial resolution derived from RTI with the overall accuracy obtained with other techniques, depth maps of different sources can be combined (MacDonald

et al. 2017). Since our aim was only to provide depth maps as an additional visual aid, such corrections were not attempted here.

Photometric stereo (Woodham 1980) is an alternative technique that also makes it possible to reconstruct a 3D model of a surface based on a set of multi-lighting images. It is primarily used in industrial machine vision applications. Photometric stereo uses the same image data as RTI, but a different technique to produce the model. Normal maps produced by photometric stereo have been shown to be of higher quality than those produced by RTI (MacDonald 2011). The applicability and the ease of use of photometric stereo as a replacement or a complementary method to inspect surface details of fossil insects should be investigated in future studies, especially considering the emergence of easily usable free software to produce the photometric stereo models (Salvant et al. 2019).

The shortcomings of RTI can be overcome with the option of using normal maps as ‘working material’ to construct high resolution models by applying focus merging to increase the depth of field and to merge normal maps to larger panoramic normal maps (‘extended field of view’). This could facilitate a more widespread adoption in paleoentomology. Even though the technique is not new, interesting new features such as the radial basis function algorithm and improved methods to virtually relight surfaces (‘neural RTI’, Dulecha et al. 2020) have been added recently to further improve the performance of RTI. This makes RTI a very useful tool to examine and document small-scale surface structures of moderately to heavily compressed insect fossils.

5. Conclusions

As already suggested by the exceptionally old age of the fossil, there is little doubt that †*Coleopsis archaica* belongs to the stem group of Coleoptera and is one of its earliest branches. Features shared with species of †Tshekardocoleidae are symplesiomorphies and therefore phylogenetically irrelevant. The retrieved data support that both taxa stand outside of a very large coleopteran subunit comprising the crown group and fossils of the late Permian, Mesozoic, and Cenozoic. A reliable documentation of structural features of fossils is essential for an adequate phylogenetic and taxonomic treatment, that should be exclusively based on apomorphies. RTI, recently still rarely used in paleoentomology, is a technique with a potential to enhance the morphological documentation and understanding of compression fossils.

6. Acknowledgements

We are very grateful to Edgar Müller (Geowissenschaftliche Sammlungen des Saarlandes) for loaning us the holotype. We also thank James H. Nebelsick (University of Tübingen) for providing access to the digital microscope, and also Oliver Betz (University of Tübingen) for support-

ing this project. Manfred Drack (University of Tübingen) is thanked for fruitful technical discussions and helpful comments on this manuscript. We thank the editor Martin Fikáček as well as two anonymous reviewers for their valuable suggestions. Thanks to the effort of numerous contributors, most of the digital work could be done using free and open source software.

7. References

- Aure X, O'Dowd PJ, Padfield J (2017) Generating 3D models of paintings through the combination of 2D, 3D and RTI data. In: Electronic Visualisation and the Arts (EVA 2017), London (UK), July 2017. <https://doi.org/10.14236/ewic/EVA2017.4>
- Béthoux O, Llamasi A, Toussaint S (2016) Reinvestigation of *Protelytron permianum* (Insecta; Early Permian; USA) as an example for applying reflectance transformation imaging to insect imprint fossils. *Fossil Record* 20(1): 1–7. <https://doi.org/10.5194/fr-20-1-2016>
- Béthoux O, Norrad RE, Stimson MR, King OA, Allen LF, Deregnacourt I, Hinds SJ, Lewis JH, Schneider JW (2021) A unique, large-sized stem Odonata (Insecta) found in the early Pennsylvanian of New Brunswick (Canada). *Fossil Record* 24(2): 207–221. <https://doi.org/10.5194/fr-24-207-2021>
- Beutel RG (1997) Über Phylogenese und Evolution der Coleoptera (Insecta). *Abhandlungen des Naturwissenschaftlichen Vereins in Hamburg* 31: 1–164.
- Beutel RG, Haas F (2000) Phylogenetic relationships of the suborders of Coleoptera (Insecta). *Cladistics* 16(1): 103–141. <https://doi.org/10.1111/j.1096-0031.2000.tb00350.x>
- Beutel RG, Ge S, Hörschemeyer T (2008) On the head morphology of *Tetraphalerus*, the phylogeny of Archostemata and the basal branching events in Coleoptera. *Cladistics* 24(3): 270–298. <https://doi.org/10.1111/j.1096-0031.2007.00186.x>
- Beutel RG, Luo X, Wipfler B (2020) Is †*Umenocoleus* a roach or a beetle (Dictyoptera or Coleoptera)? *Palaeoentomology* 3(1): 96–102. <https://doi.org/10.11646/palaeoentomology.3.1.13>
- Beutel RG, Pohl H, Yan EV, Anton E, Liu S-P, Ślipiński A, McKenna D, Friedrich F (2019) The phylogeny of Coleopterida (Hexapoda) – morphological characters and molecular phylogenies. *Systematic Entomology* 44(1): 75–102. <https://doi.org/10.1111/syen.12316>
- Beutel RG, Friedrich F, Hörschemeyer T, Pohl H, Hünefeld F, Beckmann F, Meier R, Misof B, Whiting MF, Vilhelmsen L (2011) Morphological and molecular evidence converge upon a robust phylogeny of the megadiverse Holometabola. *Cladistics* 27(4): 341–355. <https://doi.org/10.1111/j.1096-0031.2010.00338.x>
- Boudinot, BE, Yan EV, Prokop J, Beutel RG (2022) Permian parallelisms: Reanalysis of †Tshekardocoleidae sheds light on the earliest evolution of the Coleoptera. *Systematic Entomology*: 1–12. <https://doi.org/10.1111/syen.12562>
- Boute R, Hupkes M, Kollaard N, Wouda S, Seymour K, ten Wolde L (2018) Revisiting Reflectance Transformation Imaging (RTI): A tool for monitoring and evaluating conservation treatments. *IOP Conference Series: Materials Science and Engineering* 364: 012060. <https://doi.org/10.1088/1757-899X/364/1/012060>
- Brauckmann C (2007) Die Insekten im Permokarbon des Saar-Nahe-Beckens. In: Schindler T, Heidtke UHJ (Eds), *Kohlesümpfe, Seen und Halbwüsten. Dokumente einer rund 300 Millionen Jahre alten Lebewelt*. Pollichia Sonderveröffentlichung. Maierdruck, Lingenfeld, 170–196.
- Cai C, Tihelka E, Giacomelli M, Lawrence JF, Ślipiński A, Kundrata R, Yamamoto S, Thayer MK, Newton AF, Leschen RAB, Gimmel ML, Lü L, Engel MS, Huang D, Pisani D, Donoghue PCJ (2022) Integrated phylogenomics and fossil data illuminate the evolution of beetles. *Royal* 9(211771): 1–19. <https://doi.org/10.1098/rsos.211771>
- Chatzimanolis S, Grimaldi DA, Engel MS, Fraser NC (2012) *Leehermania prorova*, the earliest staphyliniform beetle, from the Late Triassic of Virginia (Coleoptera: Staphylinidae). *American Museum Novitates* 3761: 1–28. <https://doi.org/10.1206/3761.2>
- Chen SC, T'an CC (1973) A new family of Coleoptera from the Lower Cretaceous of Kansu. *Acta Entomologica Sinica* 16: 169–179.
- Cosentino A (2013) Macro photography for reflectance transformation imaging: a practical guide to the highlights method. *e-conservation Journal: autumn* 2013(1): 71–85. <https://doi.org/10.18236/econs1.201310>
- Crowson RA (1981) *The biology of the Coleoptera*. Academic Press, London, New York, 802 pp.
- Cui Y, Toussaint S, Béthoux O (2018) The systematic position of the stonefly †*culonga* Sinitshenkova, 2011 (Plecoptera: Leuctrida) reassessed using Reflectance Transforming Imaging and cladistic analysis. *Arthropod Systematics & Phylogeny* 76(2): 173–178.
- Cui Y, Brauner S, Schneider JW, Béthoux O (2022) Grylloblattidan insects from Sperbersbach and Cabarz (Germany), two new early Permian and insect-rich localities. *Journal of Paleontology* 96(2): 355–374. <https://doi.org/10.1017/jpa.2021.101>
- Demers-Potvin A, Szewdo J, Paragnani C, Larsson H (2020) First North American occurrence of hairy cicadas discovered in a Late Cretaceous (Cenomanian) exposure from Labrador, Canada. *Acta Palaeontologica Polonica* 65(1): 85–98. <https://doi.org/10.4202/app.00669.2019>
- Dulecha TG, Fanni FA, Ponchio F, Pellacini F, Giachetti A (2020) Neural reflectance transformation imaging. *The Visual Computer* 36: 2161–2174. <https://doi.org/10.1007/s00371-020-01910-9>
- Fikáček M, Beutel RG, Cai C, Lawrence JF, Newton AF, Solodovnikov A, Ślipiński A, Thayer MK, Yamamoto S (2020) Reliable placement of beetle fossils via phylogenetic analyses – Triassic *Leehermania* as a case study (Staphylinidae or Myxophaga?). *Systematic Entomology* 45(1): 175–187. <https://doi.org/10.1111/syen.12386>
- Friedrich F, Farrell BD, Beutel RG (2009) The thoracic morphology of Archostemata and the relationships of the extant suborders of Coleoptera (Hexapoda). *Cladistics* 25(1): 1–37. <https://doi.org/10.1111/j.1096-0031.2008.00233.x>
- Garrouste R, Clément G, Nel P, Engel MS, Grandcolas P, D'Haese C, Lagebro L, Denayer J, Gueriau P, Lafaute P, Olive S, Prestianni C, Nel A (2012) A complete insect from the Late Devonian period. *Nature* 488(7409): 82–85. <https://doi.org/10.1038/nature11281>
- Hammer Ø, Bengtson S, Malzbender T, Gelb D (2002) Imaging fossils using reflectance transformation and interactive manipulation of virtual light sources. *Palaeontologia Electronica* 5(4): 1–9.
- Hennig W (1950) *Grundzüge einer Theorie der phylogenetischen Systematik*. Deutscher Zentralverlag, Berlin, 396 pp.
- Hörschemeyer T, Haug JT, Béthoux O, Beutel RG, Charbonnier S, Hegna TA, Koch M, Rust J, Wedmann S, Bradler S, Willmann R (2013) Is *Strudiella* a Devonian insect? *Nature* 494(7437): E3–E4. <https://doi.org/10.1038/nature11887>
- Hughes-Hallett M, Young C, Messier P (2021) A Review of RTI and an investigation into the applicability of micro-RTI as a tool for the documentation and conservation of modern and contemporary paintings. *Journal of the American Institute for Conservation* 60(1): 18–31. <https://doi.org/10.1080/01971360.2019.1700724>

- Jäger K, Tischlinger H, Oleschinski G, Sander PM (2018) Goldfuß was right: Soft part preservation in the Late Jurassic pterosaur *Scaphognathus crassirostris* revealed by reflectance transformation imaging (RTI) and UV light and the auspicious beginnings of paleo-art. *Palaeontologia Electronica* 21.3.3T: 1–20. <https://doi.org/10.26879/713>
- Kenchington CG, Harris SJ, Vixseboxse PB, Pickup C, Wilby PR (2018) The Ediacaran fossils of Charnwood Forest: Shining new light on a major biological revolution. *Proceedings of the Geologists' Association* 129(3): 264–277. <https://doi.org/10.1016/j.pgeola.2018.02.006>
- Kim YH, Choi J, Lee YY, Ahmed B, Lee KH (2016) Reflectance transformation imaging method for large-scale objects. In: 2016 13th International Conference on Computer Graphics, Imaging and Visualization (CGiV). IEEE, Beni Mellal, Morocco, 84–87. <https://doi.org/10.1109/CGiV.2016.25>
- Kinsman T (2016) An easy to build Reflectance Transformation Imaging (RTI) system. *Journal of Biocommunication* 40(1): 10–14. <https://doi.org/10.5210/jbc.v40i1.6625>
- Kirejtshuk AG (2020) Taxonomic review of fossil coleopterous families (Insecta, Coleoptera). Suborder Archostemata: Superfamilies Coleopseioidea and Cupedoidea. *Geosciences* 10(73): 1–85. <https://doi.org/10.3390/geosciences10020073>
- Kirejtshuk AG, Nel A (2016) Origin of the Coleoptera and significance of the fossil record. *Eurasian Entomological Journal* 15(1): 66–73.
- Kirejtshuk AG, Poschmann M, Prokop J, Garrouste R, Nel A (2014) Evolution of the elytral venation and structural adaptations in the oldest Palaeozoic beetles (Insecta: Coleoptera: Tshekardocoleidae). *Journal of Systematic Palaeontology* 12(5): 575–600. <https://doi.org/10.1080/14772019.2013.821530>
- Königer S, Lorenz V, Stollhofen H, Armstrong R (2002) Origin, age and stratigraphic significance of distal fallout ash tuffs from the Carboniferous-Permian continental Saar-Nahe Basin (SW Germany). *International Journal of Earth Sciences* 91(2): 341–356. <https://doi.org/10.1007/s005310100221>
- Kotoula E, Kyranoudi M (2013) Study of ancient Greek and Roman coins using Reflectance Transformation Imaging. *e-conservation* 25: 74–88.
- Kukalová, J. (1966) Protelytroptera from the Upper Permian of Australia, with a discussion of the Protocoleoptera and Paracoleoptera. *Psyche* 73(2): 89–111.
- Lawrence JF, Ślipiński A, Seago AE, Thayer MK, Newton AF, Marvaldi AE (2011) Phylogeny of the Coleoptera based on morphological characters of adults and larvae. *Annales Zoologici* 61(1): 1–217. <https://doi.org/10.3161/000345411X576725>
- Lewis DA, Nurity M, Chatouxx H, Meriaudeau F, Mansouri A (2021) An automated adaptive focus pipeline for reflectance transformation imaging. *Electronic Imaging* 33(18): 63-1-63–7. <https://doi.org/10.2352/ISSN.2470-1173.2021.18.3DIA-063>
- Luo C-H, Beutel RG, Thomson UR, Zheng D-R, Li J-H, Zhao X-Y, Zhang H-C, Wang B (2022) Beetle or roach: systematic position of the enigmatic Umenocoleidae based on new material from Zhonggou Formation in Jiuquan, Northwest China, and a morphocladistic analysis. *Palaeoworld* 31(1): 121–130. <https://doi.org/10.1016/j.palwor.2021.01.003>
- MacDonald L, Moitinho de Almeida V, Hess M (2017) Three-dimensional reconstruction of Roman coins from photometric image sets. *Journal of Electronic Imaging* 26(1): 011017. <https://doi.org/10.1117/1.JEL.26.1.011017>
- MacDonald LW (2011) Visualising an Egyptian artefact in 3D: comparing RTI with laser scanning. *Electronic Visualisation and the Arts (EVA 2011)*: 155–162.
- Malzbender T, Wilburn B, Gelb D, Ambrisco B (2006) Surface enhancement using real-time photometric stereo. *Eurographics Symposium on Rendering*: 245–250.
- McKenna DD, Wild AL, Kanda K, Bellamy CL, Beutel RG, Caterino MS, Farnum CW, Hawks DC, Ivie MA, Jameson ML, Leschen RAB, Marvaldi AE, Mchugh JV, Newton AF, Robertson JA, Thayer MK, Whiting MF, Lawrence JF, Ślipiński A, Maddison DR, Farrell BD (2015) The beetle tree of life reveals that Coleoptera survived end – Permian mass extinction to diversify during the Cretaceous terrestrial revolution. *Systematic Entomology* 40(4): 835–880. <https://doi.org/10.1111/syen.12132>
- McKenna DD, Shin S, Ahrens D, Balke M, Beza-Beza C, Clarke DJ, Donath A, Escalona HE, Friedrich F, Letsch H, Liu S, Maddison D, Mayer C, Misof B, Murin PJ, Niehuis O, Peters RS, Podsiadlowski L, Pohl H, Scully ED, Yan EV, Zhou X, Ślipiński A, Beutel RG (2019) The evolution and genomic basis of beetle diversity. *Proceedings of the National Academy of Sciences* 116(49): 24729–24737. <https://doi.org/10.1073/pnas.1909655116>
- Misof B, Liu S, Meusemann K, Peters RS, Donath A, Mayer C, Frandsen PB, et al. (2014) Phylogenomics Resolves the Timing and Pattern of Insect Evolution. *Science* 346(6210): 763–67. <https://doi.org/10.1126/science.1257570>
- Mudge M, Malzbender T, Schroer C, Lum M (2006) New Reflection Transformation Imaging methods for rock art and multiple-viewpoint display. In: Ioannides M, Arnold D, Niccolucci F, Mania K (Eds), VAST, The 7th International Symposium on Virtual Reality, Archaeology and Cultural Heritage, Nicosia (Cyprus), November 2006, 1–9.
- Newman SE (2015) Applications of Reflectance Transformation Imaging (RTI) to the study of bone surface modifications. *Journal of Archaeological Science* 53: 536–549. <https://doi.org/10.1016/j.jas.2014.11.019>
- Ponchio F, Corsini M, Scopigno R (2019) RELIGHT: A compact and accurate RTI representation for the web. *Graphical Models* 105: 101040. <https://doi.org/10.1016/j.gmod.2019.101040>
- Ponomarenko AG (1963) Palaeozoic beetles Cupedidea of the European part of USSR. *Paleontologicheskii Zhurnal* (1): 70–85.
- Ponomarenko AG (1969) The historical development of archostematan beetles. *Trudy Paleontologicheskogo Instituta Akademiyi Nauk SSSR* 125: 1–238.
- Ponomarenko AG (1995) The geological history of beetles. *Biology, Phylogeny, and Classification of Coleoptera*. In: Pakaluk J, Ślipiński A (Eds), Papers celebrating the 80th Birthday of Roy A. Crowson. Muzeum i Instytut Zoologii PAN, Warsaw, 155–171.
- Ponomarenko AG (2000) New Beetles from the Permian of European Russia. *Paleontological Journal* 34 (Suppl. 3): S312–S316.
- Ponomarenko AG (2016) Insects during the time around the Permian—Triassic crisis. *Paleontological Journal* 50(2): 174–186. <https://doi.org/10.1134/S0031030116020052>
- Porter ST, Huber N, Hoyer C, Floss H (2016) Portable and low-cost solutions to the imaging of Paleolithic art objects: A comparison of photogrammetry and reflectance transformation imaging. *Journal of Archaeological Science: Reports* 10: 859–863. <https://doi.org/10.1016/j.jasrep.2016.07.013>
- Poschmann M, Schindler T (2004) Sitters and Grügelborn, two important Fossil-Lagerstätten in the Rotliegend (?Late Carboniferous -

- Early Permian) of the Saar-Nahe Basin (SW-Germany), with the description of a new palaeoniscoid (Osteichthyes, Actinopterygii). *Neues Jahrbuch für Geologie und Paläontologie - Abhandlungen* 232(2–3): 283–314. <https://doi.org/10.1127/njgpa/232/2004/283>
- Salvant J, Walton M, Kronkright D, Yeh C-K, Li F, Cossairt O, Katsagelos AK (2019) Photometric Stereo by UV-Induced fluorescence to detect protrusions on Georgia O’Keeffe’s paintings. In: Casadio F, Keune K, Noble P, Van Loon A, Hendriks E, Centeno SA, Osmond G (Eds), *Metal Soaps in Art: Conservation and Research*. Cultural Heritage Science. Springer International Publishing, Cham, 375–391. https://doi.org/10.1007/978-3-319-90617-1_22
- Selmo D, Sturt F, Miles J, Basford P, Malzbender T, Martinez K, Thompson C, Earl G, Bevan G (2017) Underwater reflectance transformation imaging: a technology for in situ underwater cultural heritage object-level recording. *Journal of Electronic Imaging* 26(01): 1. <https://doi.org/10.1117/1.JEL.26.1.011029>
- Tillyard RJ (1924) Upper Permian Coleoptera and a new order from the Belmont beds, New South Wales. *Proceedings of the Linnean Society of New South Wales* 49: 429–435.
- Toussaint EFA, Seidel M, Arriaga-Varela E, Hájek J, Král D, Sekerka L, Short AEZ, Fikáček M (2017) The peril of dating beetles. *Systematic Entomology* 42(1): 1–10. <https://doi.org/10.1111/syen.12198>
- Wang B, Zhang H, Jarzembowski E (2013) Early Cretaceous angiosperms and beetle evolution. *Frontiers in Plant Science* 4. Available from: <https://www.frontiersin.org/article/10.3389/fpls.2013.00360> (April 24, 2022).
- Woodham RJ (1980) Photometric method for determining surface orientation from multiple images. *Optical Engineering* 19(1): 139–144.
- Yan EV, Beutel R, Ponomarenko A (2017a) Ademosynidae (Insecta: Coleoptera): A new concept for a coleopteran key taxon and its phylogenetic affinities to the extant suborders. *Palaeontologia Electronica* (20.2.31A): 1–22. <https://doi.org/10.26879/739>
- Yan EV, Beutel RG, Ponomarenko AG (2017b) †Peltosynidae, a new beetle family from the Middle–Late Triassic of Kyrgyzstan: its affinities with Polyphaga (Insecta, Coleoptera) and the groundplan of this megadiverse suborder. *Journal of Systematic Palaeontology* 16(6): 515–530. <https://doi.org/10.1080/14772019.2017.1313789>
- Zhang S-Q, Che L-H, Li Y, Dan Liang, Pang H, Ślipiński A, Zhang P (2018) Evolutionary history of Coleoptera revealed by extensive sampling of genes and species. *Nature Communications* 9(1): 1–11. <https://doi.org/10.1038/s41467-017-02644-4>
- Zhang Z-Q (2013) Phylum Arthropoda. In: Zhang, Z.-Q. (Ed.) *Animal Biodiversity: An outline of higher-level classification and survey of taxonomic richness* (Addenda 2013). *Zootaxa* 3703(1): 17–26. <https://doi.org/10.11646/zootaxa.3703.1.6>